

# Adhesion Signals of Phospholipid Vesicles at an Electrified Interface

Nadica Ivošević DeNardis · Vera Žutić ·  
Vesna Svetličić · Ruža Frkanec

Received: 23 December 2011 / Accepted: 24 June 2012 / Published online: 19 July 2012  
© Springer Science+Business Media, LLC 2012

**Abstract** General adhesion behavior of phospholipid vesicles was examined in a wide range of potentials at the mercury electrode by recording time-resolved adhesion signals. It was demonstrated that adhesion-based detection is sensitive to polar headgroups in phospholipid vesicles. We identified a narrow potential window around the point of zero charge of the electrode where the interaction of polar headgroups of phosphatidylcholine vesicles with the substrate is manifested in the form of bidirectional signals. The bidirectional signal is composed of the charge flow due to the nonspecific interaction of vesicle adhesion and spreading and of the charge flow due to a specific interaction of the negatively charged electrode and the most exposed positively charged choline headgroups. These signals are expected to appear only when the electrode surface charge density is less than the surface charge density of the choline groups at the contact interface. In comparison, for the negatively charged phosphatidylserine vesicles, we identified the potential window at the mercury electrode where charge compensation takes place, and bidirectional signals were not detected.

**Keywords** Adhesion signal · Choline headgroup · Electrified interface · Mercury electrode · Phospholipid vesicle

## Introduction

Lipids can be classified according to their biological activity. Lipids that perform regulatory functions have a distinct residual charge distribution. Residual charge distribution is one of the factors of intermolecular recognition, leading to a specific interaction of lipid molecules with the selected proteins in various processes, particularly those involved in signal-transduction pathways (Testa et al. 1997). Charge distribution within the membrane interface determines the distribution and hydration of ions in the vicinity. Intermolecular interactions within the interface should therefore be treated as a combination of electrostatic force and hydration, along with static and dynamic steric constraints (Israelachvili 1992). The lipid composition is important for the functional requirements of the membrane. Phosphatidylcholine (PC), phosphatidylethanolamine (PE) and sphingomyelin (SM) are the most abundant lipid species in biological membranes (Gennis 1989). As the major components of the surface matrix, they determine the surface global properties that characterize its environment; but they do not interfere in membrane-associated processes, requiring them to be biologically passive. Phosphatidylserine (PS) in biological membranes plays a dual role, depending on its location. When situated on the inner surface of the plasma membrane, it interacts with a variety of proteins. The presence of PS on the plasma membrane outer surface is sporadic and has important consequences, such as in the stage preceding apoptosis (Bennet et al. 1995). Vernier and coworkers (2004) identified a specific and physiologically significant molecular event: translocation of PS from the inner leaflet of the cell membrane to the exterior face of the cell that is induced by application of ultrashort (nanosecond) and high-field (mV/m) electric pulses. One of the interesting features of the cell membrane

---

N. I. DeNardis (✉) · V. Žutić · V. Svetličić  
Ruđer Bošković Institute, P.O. Box 180, 10002 Zagreb, Croatia  
e-mail: ivosevic@irb.hr

R. Frkanec  
Institute of Immunology, P.O. Box 266, 10000 Zagreb, Croatia

is the presence of surface molecules that act like a “signature” for a cell. The interaction of protein ovalbumin and biologically active adamantyltripeptides with phospholipids in the liposomal bilayers has been described (Frkanec et al. 2003; Brgles et al. 2007).

The phospholipids deposited on a mercury electrode surface, either by extruding the drop of mercury through a monolayer spread on a gas–solution interface or by unilamellar vesicle fusion, have been extensively studied (Nelson and Benton 1986; Nelson and Auffret 1988; Leermarkers and Nelson 1990; Nelson and Leermarkers 1990; Bizzotto and Nelson 1998; Stauffer et al. 2001). Such a system can be used as a model to study the effect of an electric field on membrane stability, properties of voltage-gated membrane proteins as well as lipid–lipid and lipid–protein interactions (Guidelli et al. 2001). Mercury, with its atomically smooth surface, allows study of the surface properties of such a film and the charge transfer across a film modified by incorporated proteins (Bizzotto and Nelson 1998; Nelson and Bizzotto 1999; Guidelli et al. 2001).

The adsorption of various physical forms of PC onto a mercury electrode was extensively studied using electrochemical and optical techniques (Stauffer et al. 2001; Agak et al. 2004; Bizzotto et al. 2004). The spreading of liposomes onto the mercury surface at constant potential yields a monolayer of adsorbed PC that is identical to the layer adsorbed from the G–S interface. This monolayer undergoes several phase transitions, two of which correspond to the change in the adsorbed state and one that corresponds to the adsorption–desorption process. Nelson and Leermarkers (1990) stated that competition between the heads and the tail for access to the electrode interface was detected through the existence of a capacitance peak at the negatively charged mercury electrode. The headgroup of PS has less specific surface interaction with the mercury electrode than the PC headgroup. Thus, the conformation of PS polar heads with the two negative charges and the one positive charge on the same plane parallel to the lipid layer is not as electrostatically favored as the conformation assumed by zwitterionic lipids such as PC (Moncelli et al. 1998). Lipkowski’s group studied the behavior of phospholipid bilayers with and without the incorporated peptides in an electric field using the Au(111) electrode (Zawisza et al. 2003; Burgess et al. 2004, 2005; Xu et al. 2004; Sek et al. 2009). They found that the ingress of electrolytes is accompanied by electric field–induced changes in the orientation of the phospholipid on the electrode (Bin and Lipkowski 2006). Electroporation of membranes could be likened to the ingress of the electrolyte into the phospholipid layer at the electrode (Nelson 2010). Molecular dynamic simulation of mixed zwitterionic–anionic, asymmetric phospholipid bilayers with monovalent and divalent cations demonstrates electrostatic

and entropy-driven association of calcium and sodium ions with polar groups in the bilayer interface in terms of spatial distribution profiles and a change in the orientation of the phospholipid headgroup (Vernier et al. 2009).

While capacitance measurements in liposome suspensions generally reveal properties of the already formed monolayers at the mercury interface, time-resolved adhesion signals trace the transformation of a single liposome to a film of finite surface area. The kinetics of an adhesion event of a single liposome at the mercury electrode became accessible through signal analysis using empirical equations (Hellberg et al. 2005; Hernandez and Scholz 2006; Žutić et al. 2007) and derived analytical solutions for the reaction kinetics model (Ružić et al. 2009, 2010). The adhesion signal of a liposome reflects the dynamics of liposome adhesion by tracing the continuous transformation from the initial intact state to the intermediate deformed state and the final state of the lipid monolayer. The recently developed reaction kinetics and mechanical models (Ivošević DeNardis et al. 2012) indicate that all three states evolve simultaneously from the onset of the adhesion process. Apart from the force generated by adhesion, which drives the motion of the liposome and causes it to spread on the electrode, the main elements of the equation of motion in the mechanical model are the inertial term and the damping term associated with the release of liposome content across the membrane. The mechanical model advances the understanding of the physics of the adhesion event and offers an interpretation of the three states identified by the reaction kinetics model. In particular, it suggests that the intermediate state consists of a spherical cap containing the remaining unreleased content of the liposome and a flat annular skirt closely bound to the electrode. The main conclusion is that the liposome content is released through transient pores formed in the cap membrane.

Adhesion signals of single liposomes at the dropping mercury electrode (DME) in air-saturated suspensions were detected in a broad potential range (Ivošević DeNardis et al. 2007), while the adhesion signals recorded in deaerated liposome suspension indicated the significance of a specific interaction of phospholipid polar headgroups in close molecular contact with the mercury electrode (Žutić et al. 2007; Ivošević DeNardis et al. 2009). Here, our aim was to demonstrate that adhesion-based detection at the mercury electrode is sensitive to the polar headgroups of phospholipid vesicles. We present a study of vesicles formed from PC and PS lipids.

PC is a zwitterionic lipid, with the headgroup consisting of two oppositely charged residues: phosphate and trimethylammonium groups. On the other hand, the resulting net charge for PS is negative. PS has three residual charges: two are negative and associated with the phosphate and

carboxyl groups, while the third, positive charge, is within the ammonium group.

## Materials and Methods

The electrochemical measurement technique was based on measuring the displacement of the surface charge of the mercury electrode by adhesion and spreading of deformable particles and living cells (Žutić et al. 1993; Svetličić et al. 2000). The key ingredient in such measurement is the versatile potentiostatic control of adhesion forces by changing the surface charge and tension at the electrode–aqueous suspension interface. The adhesion force can be fine-tuned to study the interplay of the complex processes involved in a deformable particle–electrode double-layer interaction. In particular, the signature of a single adhesion event at the mercury electrode is the spike-shaped current transient (adhesion signal), which is consistent with the classical model of the electrical double-layer at the electrode–solution interface. The flow of double-layer charge displacement current reflects the dynamics of adhesive contact formation of the deformable particle with the electrode and the subsequent rupture and spreading of particle constituents to a film of the finite surface area at the millisecond time scale:

$$I_D = \frac{dA}{dt} \sigma_{12} \quad (1)$$

where  $I_D$  is the displacement current,  $A$  is the area of the interacting interface,  $t$  is time and  $\sigma_{12}$  is the surface charge density of the mercury electrode–aqueous electrolyte interface (Žutić et al. 1993). At a given potential, the current amplitude reflects the size of the adhered particle, while the signals frequency reflects the particle concentration in the suspension (Žutić et al. 1993; Svetličić et al. 2000; Ivošević DeNardis et al. 2007). The adhesion signals are defined by maximum signal amplitude ( $I_{\max}$ ), signal duration ( $\tau$ ) and displaced charge ( $q_D$ ). The displaced double-layer charge ( $q_D$ ) is obtained by integrating the area under the adhesion signal.

$$q_D = \int_{t_1}^{t_1+\tau} I dt \quad (2)$$

If a complete charge displacement takes place, as in the case of nonpolar droplets of organic liquids, the area of the contact interface ( $A_c$ ) is

$$A_c = \frac{q_D}{\sigma_{12}} \quad (3)$$

The general mechanism established for adhesion of hydrocarbon droplets and living cells is expected to be

valid as well for liposome adhesion within the wide range of surface charge densities (Ivošević DeNardis et al. 2009). Dispersion of hexadecane droplets was selected as a simple and well-defined reference system due to the fact that hexadecane is the highest saturated *n*-alkane that is fluid at room temperature and it has a large set of calculations and experimental data on surface and interfacial tension (Fowkes 1963; Ribarsky and Landman 1992). Interaction of oil droplets at the mercury–water interface is defined according to the modified Young–Dupré equation. The total Gibbs energy of interaction between a droplet and the aqueous mercury interface is

$$-\Delta G = A(\gamma_{12} - \gamma_{23} - \gamma_{13}) \quad (4)$$

where  $\gamma_{12}$ ,  $\gamma_{13}$  and  $\gamma_{23}$  are the interfacial energies at mercury–water, mercury–organic liquid and water–organic liquid interfaces, respectively. The expression in parentheses is the spreading coefficient ( $S_{132}$ ) at the three-phase boundary (Israelachvili 1992). When  $S_{132} > 0$  attachment and spreading are spontaneous processes, while when  $S_{132} < 0$  spreading is not spontaneous. The critical interfacial tension of adhesion  $(\gamma_{12})_c$  defined by  $S_{132} = 0$  will be  $(\gamma_{12})_c = \gamma_{13} + \gamma_{23}$ . In the case of nonpolar organic liquids, the critical interfacial tensions of adhesion at the positively and negatively charged interfaces are the same, showing good agreement with the calculated values (Ivošević et al. 1994, 1999) according to Young–Dupré and Good–Girifalco–Fowkes relationships (Fowkes 1962, 1963). With increasing chain length and increasing polarity of molecules, the potential range of adhesion becomes wider as the critical interfacial tension of adhesion decreases.

## Hexadecane Droplet Dispersion

The aqueous dispersion of *n*-hexadecane (99 % GC; Aldrich, Milwaukee, WI) was prepared by shaking 50  $\mu$ l of organic liquid in 250 ml of phosphate-buffered saline (PBS, 0.15 M), pH 7.47, at 300 rpm for 1 h.

## Vesicle Suspensions

1,2-Dioleoyl-*sn*-glycero-3-phosphocholine (DOPC,  $\geq 99$  %) and PS (1,2-diacyl-*sn*-glycero-3-phospho-L-serine, from bovine brain,  $\geq 97$  %) were purchased from Sigma (St. Louis, MO) and used as received. The fatty acid composition and positional distribution in glycerophosphatides of bovine gray matter are given in Yabuuchi and O'Brien (1968). Multilamellar DOPC and PS vesicles were prepared by dissolving 10 mg of lipid in 2 ml of chloroform. After rotary evaporation of the solvent, the remaining lipid film was dried in vacuum for 1 h and dispersed by gentle hand shaking in 1 ml of PBS. The solution was left

overnight at 4 °C to swell and stabilize. The suspension submitted for electrochemical measurements was characterized by a Coulter counter to determine vesicle concentration and size distribution using a 100- $\mu\text{m}$ -diameter sampling orifice tube. The normal-size distribution was fairly reproducible and stable throughout the electrochemical experiment. Vesicle suspension of  $2 \times 10^8/\text{l}$  contains predominantly size fractions in the range 3.2–16  $\mu\text{m}$ .

Unilamellar DOPC vesicle suspensions were prepared according to Moscho and coworkers (1996). The lipid was dissolved in chloroform (0.1 M), and 20  $\mu\text{l}$  of this solution was added to a 50 ml round-bottomed flask containing 920  $\mu\text{l}$  of chloroform and 150  $\mu\text{l}$  of methanol. The aqueous phase (7 ml of PBS) was carefully added along the flask walls. Organic solvents were removed in a rotary evaporator under 240–300 mmHg pressure at 40–43 °C. After evaporation for a couple of minutes, an opalescent fluid was obtained with a volume of approximately 6.5 ml. The suspension was characterized by a Coulter counter using a 140- $\mu\text{m}$ -diameter sampling orifice tube, where particle size distribution was in the range 2–60  $\mu\text{m}$ .

### Electrochemical Measurements

DME had a drop-life of 2.0 s, a flow rate of 6.0 mg/s and a maximum surface area of 4.57 mm<sup>2</sup>. All potentials were referred to an Ag/AgCl (0.1 M NaCl) reference electrode, which was separated from the measured dispersion by a ceramic frit. Its potential was +2 V versus calomel electrode (1 M KCl). Electrochemical measurements were performed using a 174A Polarographic Analyzer (Princeton Applied Research, Oak Ridge, TN) interfaced to a computer. Analogous data acquisition was performed with a DAQ card-AI-16-XE-50 (National Instruments, Austin, TX) input device, and the data were analyzed using the application developed in LabView 6.1 software (National Instruments). The current–time ( $I-t$ ) curves over 50 mercury drop lives were recorded at constant potentials, with a time resolution of 50  $\mu\text{s}$ . Signal frequency is expressed as number of adhesion event over 100 s. The aliquot of liposome suspension was added in deaerated PBS under purging with nitrogen at 25 °C.

## Results

### Hexadecane Droplets

The adhesion behavior of hexadecane droplets at the charged DME interface is presented as the dependence of signal frequency and maximum signal amplitude on electrode potential (Fig. 1). The adhesion signal frequency of

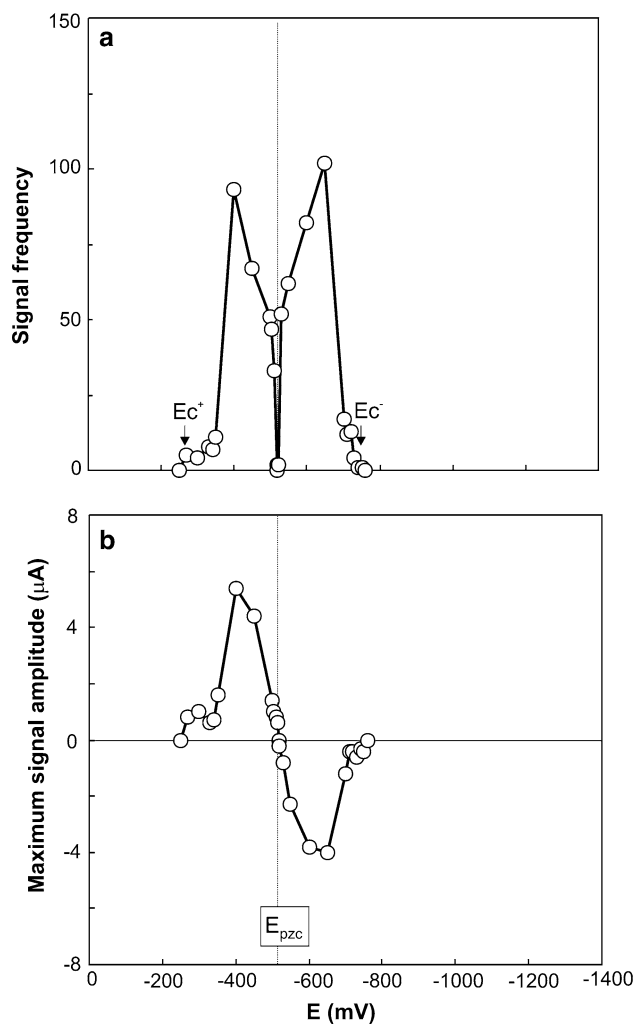


**Fig. 1** The reference system: dispersion of *n*-hexadecane droplets (180 mg/l) in PBS. Dependence of signal frequency (a) and maximum signal amplitude (b) on electrode potential.  $E_c^+$  and  $E_c^-$  denote critical potentials of adhesion at the positively and negatively charged mercury/PBS interfaces, respectively

hexadecane droplets was detected in the potential range from -270 to -730 mV in PBS. These experimentally determined potentials are referred to as critical potentials of adhesion ( $E_c^+$  and  $E_c^-$ ). The difference between the critical interfacial tensions of hexadecane adhesion at the positively and negatively charged electrodes corresponds to 1.3 mJ/m<sup>2</sup> due to the specific adsorption of chloride and phosphate anions of the supporting electrolyte at the positively charged mercury electrode (Ivošević et al. 1999). At the potentials positive to -270 mV or negative to -730 mV, adhesion of hexadecane droplets was not detected and droplets behaved as inert particles due to the stronger interaction of mercury with water and electrolyte ions than the interaction with the droplets. The signal frequency of hexadecane droplets changes by scanning the potential, creating a butterfly-shaped dependence. At the

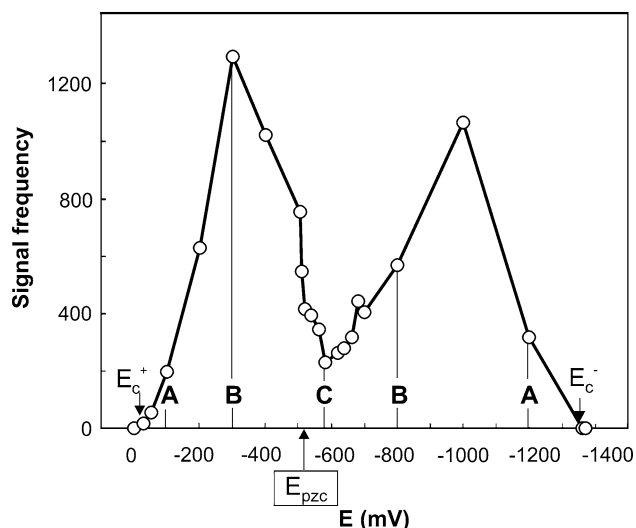


**Fig. 2** Potential dependence of the signal frequency of multilamellar DOPC vesicles in PBS. Characteristic potential points are indicated: *A* high  $\sigma_{12}$  and low  $S_{132}$  values, *B* moderate values of  $\sigma_{12}$  and  $S_{132}$  and *C* with  $\sigma_{12} < 0$  and close to the highest  $S_{132}$  values

potential of zero charge of the mercury electrode ( $E_{pzc}$ ), signal frequency is zero as there is no electrode double-layer charge to be displaced. The maximum signal amplitude of hexadecane droplets varies as well by changing the potential. The signal amplitude depends on the droplet size as well as on the polarity and the surface charge density of the mercury electrode. In particular, the signal amplitude is positive at a positively charged mercury electrode, i.e., at the potentials  $E > E_{pzc}$ . Signal amplitude displays a negative sign at a negatively charged electrode, i.e., at the potentials  $E < E_{pzc}$ . Only simple unidirectional signals of hexadecane droplets are recorded at the positively and negatively charged electrodes. At the  $E_{pzc}$  maximum signal amplitude is zero.

### Multilamellar DOPC Vesicles

The effect of the potential at the DME–PBS interface on the adhesion behavior of multilamellar DOPC vesicles in terms of signal frequency and signal shape is presented in Figs. 2 and 3. The adhesion behavior of zwitterionic DOPC vesicles differs from that of nonpolar hexadecane droplets based on (1) a wider potential range of adhesion, i.e., from  $-20$  to  $-1360$  mV; (2) signal frequency at  $E_{pzc}$ ; (3) positive direction of the signal at  $E_{pzc}$ ; (4) shifts of minimum signal frequency from  $E_{pzc}$ ; (5) critical interfacial tensions of adhesion; and (6) the appearance of bidirectional signals. The difference between the critical interfacial tensions of DOPC vesicle adhesion at the positively and negatively charged electrodes corresponds to  $27.5$  mJ/m<sup>2</sup>. The value of critical interfacial tension at the negatively charged electrode for adhesion of DOPC vesicles is significantly

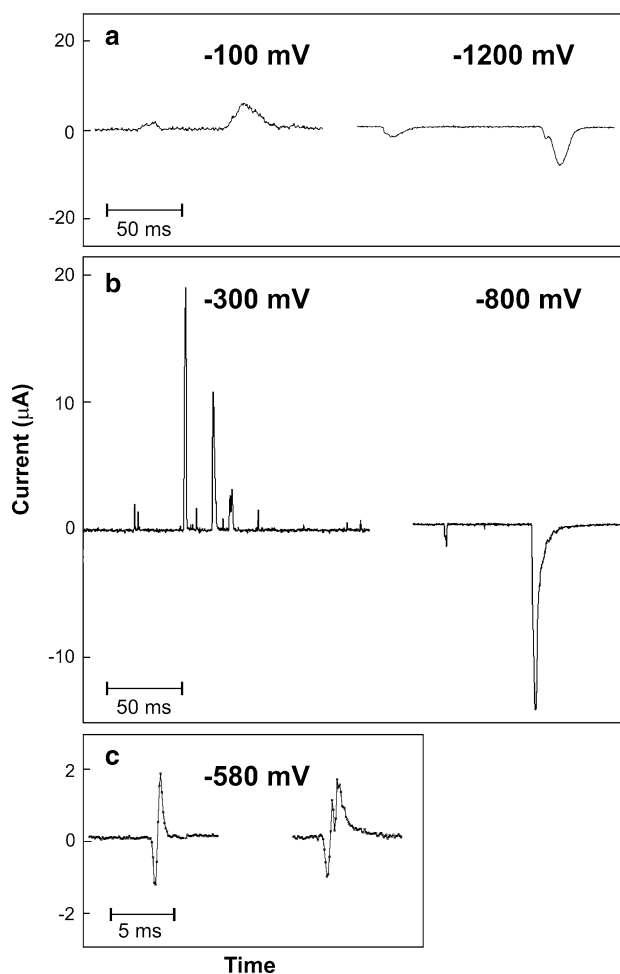


**Fig. 3** Characteristic shapes of adhesion signals at the potential points *A*, *B*, *C* defined in Fig. 2: unidirectional signals corresponding to the displacement of negative or positive charges of the electrode at **a** high  $\sigma_{12}$  but low  $S_{132}$  value and **b** moderate values of  $\sigma_{12}$  and  $S_{132}$ . Bidirectional signals occur only in a narrow potential region **c** with  $\sigma_{12} < 0$  and close to the highest  $S_{132}$  value

smaller than the value at the positively charged electrode due to the strong and specific electrostatic interaction between the positively charged choline groups and the negatively charged mercury electrode.

Figure 3 shows the selected adhesion signals of DOPC vesicles captured with a time resolution of  $50$   $\mu$ s at the selected potential points. At characteristic potential region *A* being placed in the vicinity of the critical potentials of adhesion (high  $\sigma_{12}$  and low  $S_{132}$ ), the adhesion signals show a drawn-out shape, while signal direction depends on the polarity of the surface charge of the electrode. Signal durations are in the range of  $5$ – $200$  ms at the potential of  $-100$  mV depending upon vesicle size. At potential region *B* (moderate values of  $\sigma_{12}$  and  $S_{132}$ ), adhesion signals of DOPC vesicles become sharp and narrow. Signal durations are in the range  $0.5$ – $10$  ms at the potential of  $-300$  mV. The dependence of signal duration on the spreading

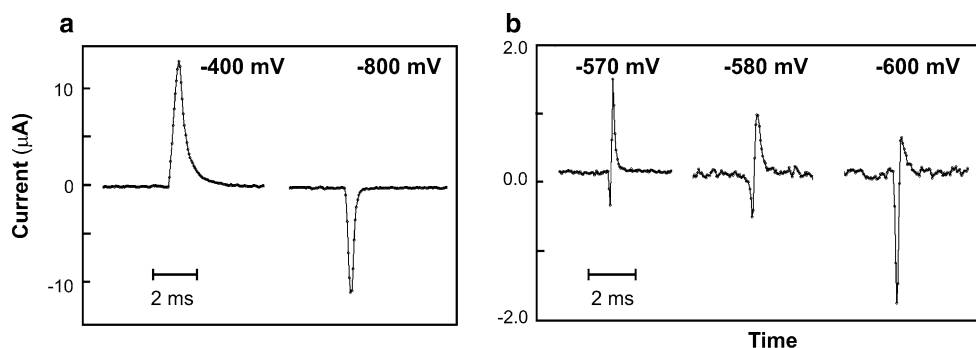


**Fig. 4** Adhesion signals of unilamellar DOPC vesicles in PBS. Unidirectional adhesion signals were recorded at  $-400$  mV ( $\sigma_{12} = 3.31 \mu\text{C}/\text{cm}^2$ ) and  $-800$  mV ( $\sigma_{12} = -7.13 \mu\text{C}/\text{cm}^2$ ) (a). Bidirectional signals were recorded at  $-570$  mV ( $\sigma_{12} = -1.85$

$\mu\text{C}/\text{cm}^2$ ),  $-580$  mV ( $\sigma_{12} = -2.09 \mu\text{C}/\text{cm}^2$ ) and  $-600$  mV ( $\sigma_{12} = -2.59 \mu\text{C}/\text{cm}^2$ ), i.e., potential region with  $\sigma_{12} < 0$  and close to the highest  $S_{132}$  (b)

coefficient was determined for hydrocarbon droplets irrespective of the polarity of the electrode charge, proving that interfacial energy governs the rate of spreading (Ivošević and Žutić 2002). Only simple unidirectional signals of DOPC vesicles are recorded at potential regions A and B. At potential region C (with  $\sigma_{12} < 0$  and close to the highest  $S_{132}$ ), complex bidirectional signals of DOPC vesicles were recorded only in a narrow potential range.

#### Unilamellar DOPC Vesicles

We performed closer examination of the adhesion behavior of PC vesicles by scanning the electrode potential in a suspension of unilamellar DOPC. In general, the potential range of adhesion at the DME and the adhesion signal feature in suspension of unilamellar DOPC resemble those recorded in the suspension of multilamellar DOPC. Figure 4a illustrates the shape of adhesion signals and the direction of flow of the compensating current at the positive and negative surface charge densities, respectively. The smallest signal of DOPC vesicles measured at the potential of  $-400$  mV that is detected beyond the noise level has an amplitude of  $0.18 \mu\text{A}$ , signal duration of  $1$  ms and displaced charge of  $49$  pC, which corresponds to the contact area of  $1484 \mu\text{m}^2$ . This signal was recorded at a drop lifetime of the mercury electrode of  $0.26$  s, and the resulting portion of occupied electrode surface area is  $0.13\%$ . If the surface area of the DOPC molecule in the bilayer ( $72.5 \text{ \AA}$ ) (Lagüe et al. 2001) is the same as in the monolayer on the positively charged electrode with the hydrophobic tails oriented perpendicularly to the electrode, the radius of the unilamellar vesicle in solution would be  $7 \mu\text{m}$ . However, in the case of multilamellar vesicles, only the radius of an equivalent unilamellar vesicle could be evaluated from the displaced charge, assuming a successive peel off, rupture and spreading of bilayers to the phospholipid monolayer, which is the only stable structure

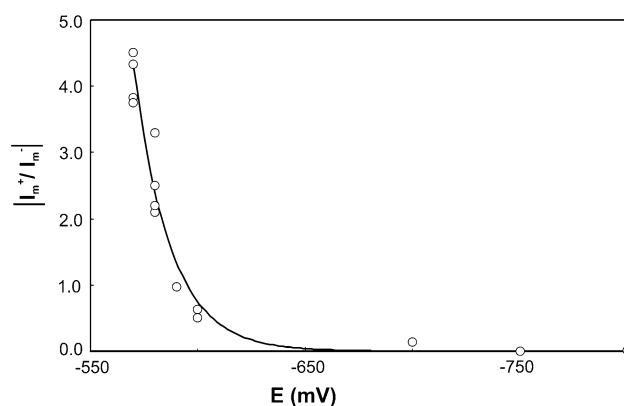


**Fig. 5** Potential dependence of peak heights ratio  $|I_m^+ / I_m^-|$  of bidirectional signals of unilamellar DOPC vesicles in PBS

at the aqueous mercury interface at potentials of strong adhesion.

Scanning the electrode potential around  $E_{pzc}$  (potential region C) reveals the characteristic bidirectional adhesion signals (Fig. 4b). Bidirectional signals of DOPC vesicles appear in the narrow potential range from  $-570$  to  $-700$  mV, which corresponds to a surface charge density  $-1.85 \geq \sigma_{12} \geq -5.08$ . This type of adhesion signal was first reported for multilamellar egg-PC liposomes, showing that bidirectional signals originate from a specific interaction of positively charged choline groups of phospholipid polar heads when in immediate contact with the negatively charged mercury electrode (Žutić et al. 2007). Here, we show that the phenomenon of bidirectional signals is characteristic of PC vesicles irrespective of their lamellarity. We confirmed the appearance of bidirectional signals of vesicles around the  $E_{pzc}$  of the mercury electrode as well as in the systems of DMPC vesicles in PBS at  $25^\circ\text{C}$  and DPPC vesicles in PBS at  $45^\circ\text{C}$  (Ivošević et al. 2009). The ratio of the positive portion peak to the negative portion peak of the bidirectional signal shows potential

dependence (Fig. 5). Attenuation of the positive portion peak with increasing negative potential is due to the charge flow associated with vesicle spreading, which dominates over the charge flow associated with a specific interaction of choline groups.

### Multilamellar PS Vesicles

The effect of potential at the DME on the adhesion behavior of multilamellar PS vesicles in terms of signal frequency was examined in potential region C, to trace a specific behavior of the serine polar headgroup. The behavior observed was quite different from that of the choline group, which is characterized by bidirectional signals. Although PS adhesion signals had the same appearance for potential regions A and B, no signals were observed in region C, i.e., in the range from  $-520$  to  $-560$  mV (Fig. 6). At pH 7.5 the polar head of PS is negatively charged (Moncelli et al. 1998). The absence of adhesion signals more negative than  $E_{pzc}$  indicated overall interaction of the positively charged vesicles. Since measured double-layer charge displacement takes place at a distance of less than  $10$  Å, it is possible to detect the charge corresponding to the ammonium group. Kotyńska and Figaszewski (2005) studied the effect of the adsorption of ions ( $H^+$ ,  $Na^+$ ,  $OH^-$ ,  $Cl^-$ ) present in the solution upon the electric charge of the liposome membrane formed of PC vesicles. The surface charge density of the membrane was determined as a function of pH and of electrolyte concentration obtained with electrophoretic mobility measurements. For high concentration of sodium chloride (0.1 M) at pH 7, competition in the adsorption between the

$H^+$  and  $Na^+$  ions takes place. The increase in  $Na^+$  ion concentration causes a decrease in the negative charge, proving the adsorption of  $Na^+$ . The confined range of surface charge densities of the mercury electrode in which electrostatic interaction was identified is from  $-0.55$  to  $-1.50$   $\mu C/cm^2$ . Our results are in agreement with the capacitance measurements, where the determined charge density on PS-coated mercury electrode in 0.1 M KCl at constant applied potential of  $-0.5$  V/vs. SCE and at pH 7.5 was around  $-0.49$   $\mu C/cm^2$  (Moncelli et al. 1998).

### Discussion

The bidirectional signal is composed of the charge flow due to the nonspecific charge displacement at the initial contact of a liposome with the electrode (negative portion of the signal) and of the charge flow due to a specific interaction of positively charged choline groups of phospholipid polar heads that form a direct contact with the electrode surface (positive portion of the signal). The lipid vesicle first establishes the adhesion contact through displacement of the ions situated in the inner Helmholtz plane (IHP, the initial negative portion of the peak) in such a way that the polar headgroups of still intact vesicles come in direct (molecular) contact with the mercury electrode and charge transfer takes place due to a specific electrostatic interaction of the positively charged choline groups of phospholipids and the negatively charged electrode, forming a surface complex with a partial charge transfer (positive portion of the peak). With increasing negative potential, the compensating charge flow due to the spreading of vesicle dominates over the charge flow due to a specific electrostatic interaction of choline groups because the increased surface charge density of the electrode compensates for the positive charge. For potentials where the electrode surface charge is close to, equal to or exceeds the charge density created by the choline groups, the positive portion of the bidirectional signal attenuates and finally disappears.

Our interpretation of the bidirectional signal origin is in agreement with studies of potential-dependent fluorescence of DOPC on the mercury surface by Stoodley and Bizzotto (2003). They provided evidence of polar lipid headgroup–mercury electrode interaction based on fluorescein chromophores residing in the lipid headgroup/aqueous region. Around the  $E_{pzc}$  lipids are closer to the electrode and form the preadsorbed state, effectively quenching fluorescence. By scanning the potential negatively from the  $E_{pzc}$ , fluorescence increases and the lipid layer desorbs and remains close to the electrode surface. High affinity of tetraalkylammonium cations for interaction with the negatively charged mercury electrode is well known in the electrochemical literature (Ryan et al. 1987). Choline methyl

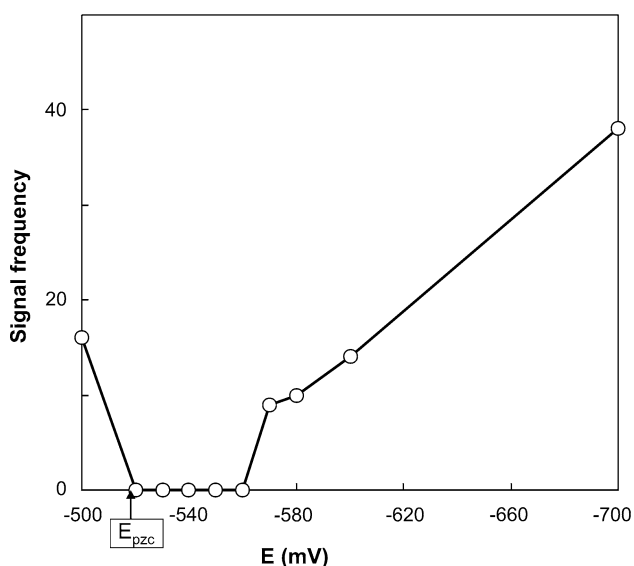


**Fig. 6** Potential dependence of signal frequency of multilamellar PS vesicles in PBS

groups are hydrophobic, and adjacent water molecules are hydrogen-bonded between themselves, forming a clathrate shell around the PC headgroup. It is estimated that about 25–30 water molecules are needed to fully hydrate the choline headgroup (Damodaran and Merz 1993, 1994). The lack of hydrogen bonds enables the choline moiety to rotate freely (Israelachvili 1992). The range of the surface charge densities where specific electrostatic interaction of choline and mercury electrode was identified is from  $-1.85$  to  $-5.08 \mu\text{C}/\text{cm}^2$ . The  $\sigma_{12}$  value at which the positive portion of the bidirectional signal disappears is the surface charge density of the mercury electrode needed to compensate for the charge of the choline groups. From this value, we can calculate the area at the electrode surface occupied by one positive charge of the choline group, which corresponds to  $315 \text{ \AA}^2$ . This indicates a flat orientation of lipid molecule in the monolayer formed after liposome spreading over the electrode, although some other orientations of PC lipid molecule at the mercury electrode have been proposed (Hellberg et al. 2005; Hernandez and Scholz 2006; Nelson 2010).

Another piece of evidence for such an orientation of lipid molecules at the negatively charged electrode is found by analysis of the adhesion signal of a single DMPC liposome (Hernandez and Scholz 2006), where for the unilamellar liposome the surface area occupied by one lipid molecule in the monolayer is  $230 \text{ \AA}^2$  compared to the surface area occupied by a headgroup, which equals  $65 \text{ \AA}^2$ . In the pH range 4–9, the PC film is uncharged and does not contain partially protonated ionizable groups. Over this pH range the conformation of the PC polar head with the P-N dipoles aligned head to tail in the direction parallel to the monolayer is the most energetically favored arrangement from the electrostatic viewpoint (Moncelli et al. 1998).

Finally, the orientation of DMPC molecules at the Au(111) electrode surface observed at a charge density close to zero was visualized by STM with high molecular resolution. The images of flat-lying DMPC molecules with acyl chains oriented parallel to the surface and assembled into an oriented monolayer could be observed in dilute vesicle solution but only during a short period of time after vesicle deposition. With time, the molecules reorient and the monolayer is transformed into a hemimicellar film (Xu et al. 2004).

## Conclusions

We demonstrated that adhesion-based detection is sensitive to polar headgroups in phospholipid vesicles. By studying the effect of potential on adhesion signals of PC and PS vesicles at the DME, we have identified the potential window of the interaction of lipid polar headgroups with

the substrate. Thus, for PC vesicles the interaction is manifested in the form of bidirectional signals. The bidirectional signal is composed of (1) the charge flow due to vesicle adhesion and spreading (displacement of ions from the electrode IHP), yielding the negative portion of bidirectional signal, and (2) the charge flow due to a specific interaction of the negatively charged electrode and the most exposed charged group of the phospholipid polar head, i.e., the positively charged trimethylammonium group, yielding the positive portion of the bidirectional signal. Therefore, bidirectional signals are expected to appear only when the electrode surface charge density is less than the surface charge density of the choline groups at the contact interface.

We conclude that the major distinction between phospholipid vesicles and oil droplets is manifested as (1) the difference between the critical interfacial tensions of adhesion at the positively and negatively charged electrodes, (2) the appearance of specific bidirectional signals at the low surface charge density and (3) the molecular orientation in the monolayer. In order to derive molecular-level imaging and to gain information about the phospholipid orientation with respect to the potential stimuli, further research should employ computer simulation methods to model such a membrane system.

**Acknowledgements** This study was supported by the Croatian Ministry of Science, Education and Sports, projects 098-0982934-2744 and 021-0212432-2431. Special thanks are due to Ivica Ružić for help with charge density calculations.

## References

- Agak JO, Stoodley R, Retter U, Bizzotto D (2004) On the impedance of a lipid-modified Hg/electrolyte interface. *J Electroanal Chem* 562:135–144
- Bennet MR, Gibson DF, Schwartz SM, Tait JF (1995) Binding and phagocytosis of apoptotic vascular smooth muscle cells is mediated in part by exposure of phosphatidylserine. *Circ Res* 77:1136–1145
- Bin X, Lipkowski J (2006) Electrochemical and PM-IRRAS studies of the effect of cholesterol on the properties of the headgroup of a DMPC bilayer supported at a Au(111) electrode. *J Phys Chem B* 110:26430–26441
- Bizzotto D, Nelson A (1998) Continuing electrochemical studies of phospholipid monolayers of dioleoyl phosphatidylcholine at the mercury–electrolyte interface. *Langmuir* 14:6269–6273
- Bizzotto D, Yang Y, Shepherd JL, Stoodley R, Agak J, Stauffer V, Lathuilliere M, Akhtar AS, Chung E (2004) Electrochemical and spectroelectrochemical characterization of lipid organization in an electric field. *J Electroanal Chem* 574:167–184
- Brgles M, Miroslavljević K, Noethig-Laslo V, Frkanec R, Tomašić J (2007) Spin-labelling study of interactions of ovalbumin with multilamellar liposomes and specific anti-ovalbumin antibodies. *Int J Biol Macromol* 40:312–318
- Burgess I, Li M, Horswell SL, Szymanski G, Lipkowski J, Majewski J, Satija S (2004) Electric field-driven transformations of a



- supported model biological membrane—an electrochemical and neutron reflectivity study. *Biophys J* 86:1763–1776
- Burgess I, Li M, Horswell SL, Szymanski G, Lipkowski J, Satija S, Majewski J (2005) Influence of the electric field on a biomimetic film supported on a gold electrode. *Colloids Surf B* 40:117–122
- Damodaran KV, Merz KM (1994) A comparison of DMPC- and DLPE-based lipid bilayers. *Biophys J* 66:1076–1087
- Damodaran KV, Merz KM (1993) Headgroup–water interactions in lipid bilayers: a comparison between DMPC- and DLPE-based lipid bilayers. *Langmuir* 9:1179–1183
- Fowkes FM (1962) Ideal two-dimensional solutions. III. Penetration of hydrocarbons in monolayers. *J Phys Chem* 66:1863–1866
- Fowkes FM (1963) Additivity of intermolecular forces at interfaces. I. Determination of the contribution to surface and interfacial tensions of dispersion forces in various liquids. *J Phys Chem* 67:2538–2541
- Frkanec R, Noethig Laslo V, Vranešić B, Miroslavljević K, Tomašić J (2003) A spin labelling study of immunomodulating peptidoglycan monomer and adamantyltripeptides entrapped into liposomes. *Biochim Biophys Acta* 1611:187–196
- Gennis RB (1989) *Biomembranes: molecular structure and function*. Springer, Heidelberg
- Guidelli R, Aloisi G, Becucci L, Dolfi A, Monicelli R, Buoninsegni FT (2001) Bioelectrochemistry at metal–water interfaces. *J Electroanal Chem* 504:1–28
- Hellberg D, Scholz F, Schubert F, Lovrić M, Omanović D, Hernandez VA, Thede R (2005) Kinetics of liposome adhesion on a mercury electrode. *J Phys Chem B* 109:14715–14726
- Hernandez VA, Scholz F (2006) Kinetics of the adhesion of DMPC liposomes on a mercury electrode: effect of lamellarity, phase composition, size and curvature of liposomes and presence of the pore forming peptide mastoparan X. *Langmuir* 22:10723–10731
- Israelachvili JN (1992) *Intermolecular forces & surface forces*. Academic Press, New York
- Ivošević DeNardis N, Žutić V, Svetličić V, Frkanec R, Tomašić J (2007) In situ amperometric characterization of liposome suspensions with concomitant oxygen reduction. *Electroanal* 19:2444–2450
- Ivošević DeNardis N, Žutić V, Svetličić V, Frkanec R (2009) Amperometric adhesion signals of liposomes, cells and droplets. *Chem Biochem Eng Q* 23:87–92
- Ivošević DeNardis N, Ružić I, Pečar-Ilić J, El Shawish S, Zihelr P (2012) Reaction kinetics and mechanical models of liposome adhesion at charged interface. *Bioelectrochemistry* 88:48–56
- Ivošević N, Žutić V (2002) Effect of electrical potential on adhesion, spreading and detachment of organic droplets at an aqueous electrolyte/metal interface. In: Mittal K (ed) *Contact angle, wettability and adhesion*. VSP, Zeist, pp 549–561
- Ivošević N, Tomaić J, Žutić V (1994) Organic droplets at an electrified interface: critical potentials of wetting measured by polarography. *Langmuir* 10:2415–2418
- Ivošević N, Žutić V, Tomaić J (1999) Wetting equilibria of hydrocarbon droplets at an electrified interface. *Langmuir* 15:7063–7068
- Kotyńska J, Figaszewski ZA (2005) Adsorption equilibria between liposome membrane formed phosphatidylcholine and aqueous sodium chloride solution as a function of pH. *Biochim Biophys Acta* 1720:22–27
- Lagüe P, Zuckermann MJ, Roux B (2001) Lipid-mediated interactions between intrinsic membrane proteins: dependence on protein size and lipid composition. *Biophys J* 81:276–284
- Leermakers FAM, Nelson A (1990) Substrate-induced structural changes in electrode-adsorbed lipid layers: a self-consistent field theory. *J Electroanal Chem* 278:53–72
- Monicelli MR, Becucci L, Tadini Buoninsegni F, Guidelli R (1998) Surface dipole potential at the interface between water and self-assembled monolayers of phosphatidylserine and phosphatidic acid. *Biophys J* 74:2388–2397
- Moscho A, Orwar O, Chiu DT, Modi BP, Zare RN (1996) Rapid preparation of giant unilamellar vesicles. *Proc Natl Acad Sci USA* 93:11443–11447
- Nelson A (2010) Electrochemistry of mercury supported phospholipid monolayers and bilayers. *Curr Opin Colloid Interface Sci* 15:455–466
- Nelson A, Auffret N (1988) Phospholipid monolayers of di-oleoyl lecithin at the mercury/water interface. *J Electroanal Chem* 244:99–113
- Nelson A, Benton A (1986) Phospholipid monolayers at the mercury/water interface. *J Electroanal Chem* 202:253–270
- Nelson A, Bizzotto D (1999) Chronoamperometric study of TI(I) reduction at gramacidin-modified phospholipid-coated mercury electrodes. *Langmuir* 15:7031–7039
- Nelson A, Leermakers FAM (1990) Substrate-induced structural changes in electrode-adsorbed lipid layers: experimental evidence from the behavior of phospholipid layers on the mercury–water interface. *J Electroanal Chem* 278:73–83
- Ribarsky MW, Landman U (1992) Structure and dynamics of *n*-alkanes confined by solid surfaces. I. Stationary crystalline boundaries. *J Chem Phys* 97:1937–1949
- Ružić I, Ivošević DeNardis N, Pečar-Ilić J (2009) Kinetics of the liposome adhesion on a mercury electrode: testing of a mathematical model. *Int J Electrochem Sci* 4:787–793
- Ružić I, Pečar-Ilić J, Ivošević DeNardis N (2010) Mathematical model for kinetics of organic particle adhesion at an electrified interface. *J Electroanal Chem* 642:120–126
- Ryan CM, Svetličić V, Kariv-Miller E (1987) Electrogenerated R<sub>4</sub>N(Hg)<sub>5</sub> films: stoichiometry and substituent effects. *J Electroanal Chem* 219:247–258
- Sek S, Laredo T, Dutcher JR, Lipkowski J (2009) Molecular recognition imaging of an antibiotic peptide in a lipid matrix. *J Am Chem Soc* 131:6439–6444
- Stauffer V, Stoodley R, Agak JO, Bizzotto D (2001) Adsorption of DOPC onto Hg G/S interface a liposomal suspension. *J Electroanal Chem* 516:73–82
- Stoodley R, Bizzotto D (2003) Epi-fluorescence microscopic characterization of potential-induced changes in a DOPC monolayer on a Hg drop. *Analyst* 128:552–561
- Svetličić V, Ivošević N, Kovač S, Žutić V (2000) Charge displacement by adhesion and spreading of a cell: amperometric signals of living cells. *Langmuir* 16:8217–8220
- Testa B, Kier LB, Carrupt PA (1997) A system approach to molecular structure, intermolecular recognition, and emergence-dissolvence in medical research. *Med Res Rev* 17:303–326
- Vernier PT, Sun Y, Marcu L, Craft CM, Gundersen M (2004) Nano-electropulse-induced phosphatidylserine translocation. *Biophys J* 86:4040–4048
- Vernier PT, Ziegler MJ, Dimova R (2009) Calcium binding and headgroup dipole angle in phosphatidylserine–phosphatidylcholine bilayers. *Langmuir* 25:1020–1027
- Xu S, Szymanski G, Lipkowski J (2004) Self-assembly of phospholipid molecules at a Au(111) electrode surface. *J Am Chem Soc* 126:12276–12277
- Yabuuchi H, O'Brien JS (1968) Positional distribution of fatty acids in glycerophosphatides of bovine grey matter. *J Lipid Res* 9:65–67
- Zawisza I, Lachenwitzer A, Zamlyny V, Horswell SL, Goddard JD, Lipkowski J (2003) Electrochemical and photon polarization modulation infrared reflection absorption spectroscopy study of the electric field driven transformations of a phospholipid bilayer supported at a gold electrode surface. *Biophys J* 85:4055–4075

Žutić V, Kovač S, Tomaić J, Svetličić V (1993) Heterocoalescence between dispersed organic microdroplets and a charged conductive interface. *J Electroanal Chem* 349:173–186

Žutić V, Svetličić V, Hozic Zimmermann A, Ivošević DeNardis N, Erkanec R (2007) Comment on “liposomes on a mercury

electrode. effect of lamellarity, phase composition, size and curvature of liposomes, and presence of the pore forming peptide mastoparan X”. *Langmuir* 23:8647–8649